Available online at www.sciencedirect.com
SCIENCE DIRECT®
European Journal of Mechanics B/Fluids 23 (2004) 781–794

Mixed buoyant-Marangoni convection due to dissolution of a droplet in a liquid–liquid system with miscibility gap

Marcello Lappa *, Chiara Piccolo, Luigi Carotenuto

MARS (Microgravity Advanced Research and Support Center), Via Emanuele Gianturco 31, 80142 Napoli, Italy

Received 3 July 2003; received in revised form 26 January 2004; accepted 12 February 2004

Available online 9 April 2004

Abstract

Fluid flows occurring during solidification of metal alloys influence the composition and the properties of the final solid. Transport phenomena for this process are investigated using a model system: a dissolving drop inside a surrounding liquid under a thermal gradient. Experiments are performed with transparent organic liquids with miscibility gap. Novel mathematical models and numerical strategies are presented to correlate experimental results and in particular to explain the behaviour of stable and unstable solutal plumes that are formed above the dissolving droplet.

Keywords: Dissolution process; Miscibility gap; Buoyancy and Marangoni convection

1. Introduction

In recent years binary immiscible liquid–liquid systems, and partially miscible liquid pairs, have been finding increasing interest in fundamental studies of interphase mass transfer due to their relevance for technological applications. This relevance is motivated in particular by problems related to the separation of alloys, where a number of different phenomena dealing with the dynamics of dispersed particles occur (drops coalescence and wetting, sedimentation and flotation, Marangoni migration, etc.).

For this case, in fact, the two-phase liquid consists of dispersed drops in a matrix liquid and the quality of the dispersion alloys is defined by the degree of homogeneity of the minority phase distribution. It is well known that the strength of the metal alloys can be improved if a uniform dispersion of fine particles in the matrix is achieved [1].

Optimization of the metal alloy therefore can be seen as a matter of searching, as systematically as possible, the conditions that lead to the aforementioned uniform dispersion of the drops. In practice this corresponds to study the effects that can move the system away from the desired condition. The detailed knowledge of such effects may help researchers in preventing them.

For instance in the presence of gravity field (i.e., on ground), as the density of the phases is different, the minority phase may experience buoyancy (Prinz and Romero [2]), i.e., rapid separation of the alloy components may occur through sedimentation or flotation.

Superimposed on this is the fact that during alloy solidification, the melt is subject to temperature gradients. These gradients can be responsible for several additional complex and intriguing phenomena. In a gravity field, they lead in most cases to buoyancy driven convective flows and regardless of the presence of gravity (i.e., also under microgravity conditions) they can produce Marangoni stress at the interface between the two liquids.

* Corresponding author. Via Salvator Rosa 53, San Giorgio a Cremano, 80046 Napoli, Italy.
E-mail address: marlappa@marscenter.it, marlappa@unina.it, lappa@marscenter.it (M. Lappa).

0997-7546/$ – see front matter
doi:10.1016/j.euromechflu.2004.02.001

These stresses in turn are responsible for important phenomena known as “wetting and coalescence prevention”. Non-coalescence of drops due to Marangoni convection was observed for the first time during the Spacelab mission D2 (1992). Following this observation a number of theoretical, numerical and experimental studies was initiated on ground that have shown that both non-coalescence and non-wetting are caused by Marangoni flows that entrain surrounding fluid in the gap between two drops (or one drop and a solid surface) forming an immiscible fluid film that prevents intimate contacts between molecules that belong to the adjacent surfaces (see, e.g., [3–6]). These mechanisms are expected to play a very important role in the aforementioned dynamics of solidifying alloys with a minority phase dispersed in an immiscible external liquid matrix.

Marangoni stresses are also responsible for another important effect, the so-called “Marangoni migration”: due to the surface Marangoni stress distribution induced by thermal effects, free liquid drops surrounded by an immiscible liquid migrate towards the hot region. For this reason often the anticipated structure of uniformly distributed intrusions of the minority phase in the external matrix after solidification does not occur even if the experiments are carried out under microgravity conditions. Many authors have studied in detail this aspect in the case of immiscible liquids (see, e.g., Young, Goldenstein and Block [7], Subramanian and Balasubramaniam [8], Subramanian [9]).

Despite the above-mentioned different worthy contributions to the understanding of the behaviour and the dynamics of the liquid–liquid systems as model of industrial solidification processes, however there are still many aspects that need further investigation. One of these, probably one of the most relevant, deals with the fact that actually real liquid–liquid alloys systems are not immiscible but exhibit a so-called miscibility gap [1].

A miscibility gap in the liquid phase is also found in many other different systems: binary mixtures of organic liquids, sulphides and silicates systems, glasses and liquid crystals. Further to the case of metal alloys, many industrial applications and processes are based on miscibility gap and related phenomena.

In the light of the above arguments and according to the major difficulty in investigating liquid metals for their opaqueness, organic liquids are often used as model substances to study the flow and the solidification of alloys. For instance, Methanol and Cyclohexane have been selected and investigated both in Earth and in Space laboratories since they are transparent liquids exhibiting a miscibility gap in the phase diagram; in addition, the small difference in density (0.769 [g/cm^3] the Cyclohexane, 0.782 [g/cm^3] the Methanol) allows one, in principle, to minimize buoyancy and sedimentation effects.

The thermo-solutal-capillary migration of a dissolving liquid drop, initially composed of pure Methanol, injected in a closed cavity filled of (initially) pure Cyclohexane with differentially heated end walls under microgravity conditions was studied by Bassano [10] using a finite-volume formulation and a level-set technique. The main goal of the analysis, with respect to previous analyses dealing with immiscible liquids, was to clarify at what extent the thermally-induced drop migration is affected by the dissolution process.

It is worthwhile to stress how, however, the behaviour of dissolving drops in a miscible matrix is even more interesting in the case of normal gravity conditions, the industrial processes being usually carried out on ground. Under normal gravity conditions the dissolution of dispersed drops leads to solutal “pluming phenomena” that may exhibit a very intriguing behaviour. These aspects are the subject of the present analysis.

2. Experiments

The couple of liquids exhibiting a first order phase transition used for the simulations is Cyclohexane (C_6H_{12})-Methanol (CH_3OH). This couple has been selected since: (i) as previously discussed the components have nearly the same density; (ii) are transparent, allowing both the direct visualization of the drop and the use of optical and interferometric diagnostic devices; (iii) their mixture has a critical temperature of 45.7 °C, slightly larger than the ambient one. The Cyclohexane-Methanol equilibrium curve is given in Fig. 1.

The experiments have been performed using a cell made of quartz, 1 [cm] × 1 [cm] × 4 [cm], filled with liquid. The droplet is formed at the tip of a capillary having diameter = 1 mm (see Fig. 2). The experiments are carried out injecting Methanol from the bottom side of the test cell and the cell is filled by Cyclohexane. The drop is anchored to the position of the needle (or capillary tube) used to inject the liquid into the matrix.

The temperature of the system is controlled by Peltier elements at the top and bottom walls.

The experimental procedure includes the direct visual observation of the droplet and an interferometric analysis performed to analyze the concentration field and therefore the mass transfer at the liquid–liquid interface. In particular a Wollaston lateral shearing interferometer [Malacara] has been used to analyze refraction index gradients: fringes correspond to the locations having equal values of the component of gradient along the shearing direction. The variation of gradient along the shearing direction related to consecutive fringes is given by $\lambda/L\delta$, λ being the wavelength, L the cell thickness and δ the shearing distance. By rotating the Wollaston prism by 90° horizontal and vertical shearing can be obtained; for the experiment, in practice the direction is horizontal, being the problem axi-symmetric along the capillary axis. The light source is a diode laser,

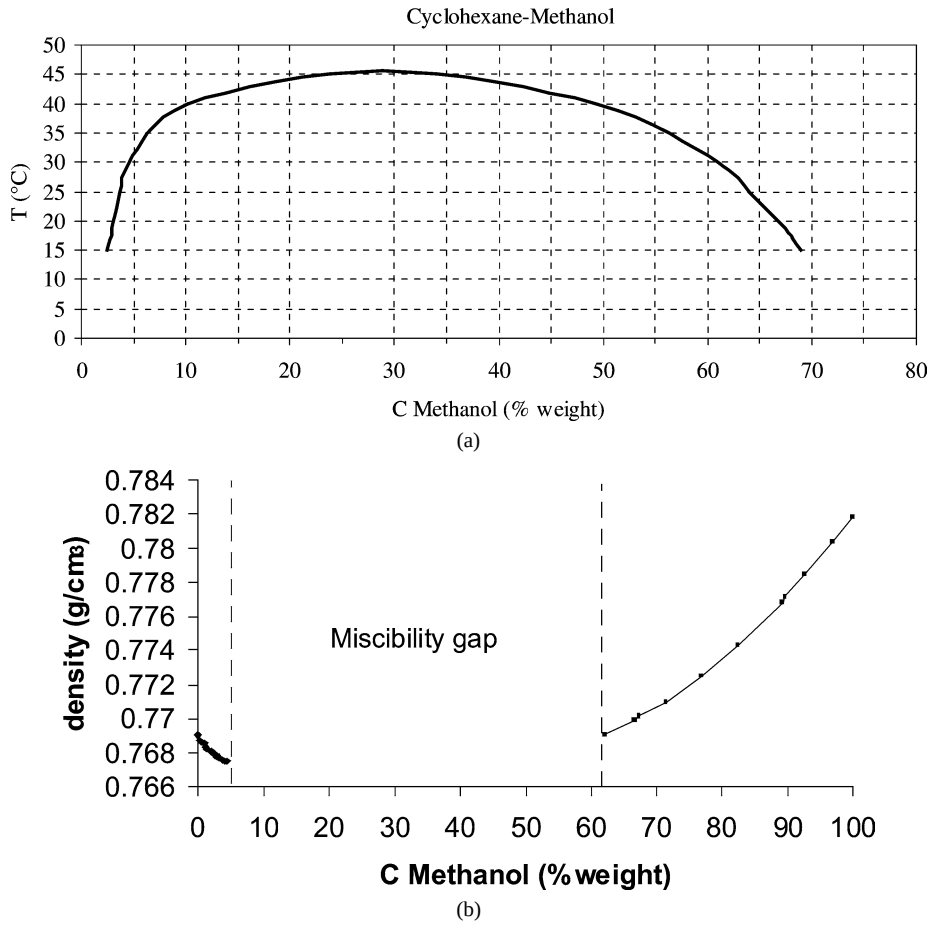

Fig. 1. Phase diagram (a) and density versus Methanol concentration (b) for the Cyclohexane–Methanol system.

$\lambda = 638.6$ nm (Micro Laser Systems) and the wave-front deformation of the cell's quartz walls amounts to λ in order to reduce optical aberrations.

A digital camera (Hamamatsu) also has been used, having a sensor area of 8.58×8.58 mm^2, and a resolution of 1024×1280 pixels.

Hereafter the drop liquid will be denoted as phase 1 and the liquid matrix as phase 2.

3. Numerical model

3.1. Basic assumptions

Fig. 2(a) shows the geometry of the problem. A thermodynamic constraint fixes the concentration jump between the interface sides. This jump, together with that of the concentration normal derivatives, in turn defines the entity of the dissolution cross-flow through the interface and the interface velocity relative to fluid.

The liquids are assumed with constant phase density and transport coefficients. The drop is bounded by a spherical liquid/liquid interface whose radius changes in time due to growth or dissolution. The hypothesis of spherical surface is acceptable if zero-g conditions prevail or, on the ground, if the volume of the liquid drop is small (few millimetres) and/or if the density difference between the two phases is very small (present case).

3.2. Moving boundary method

In a phase-field model, a phase-field variable ϕ which varies in space and time is introduced to characterize the phase. In place of the 'sharp' transition from one phase to the other the phase-field varies smoothly but rapidly through an interfacial region. The effect is a formulation of the free boundary problem that in principle does not require application of interfacial conditions at the unknown location of a phase boundary. This formulation is at the root of the most recent and popular methods

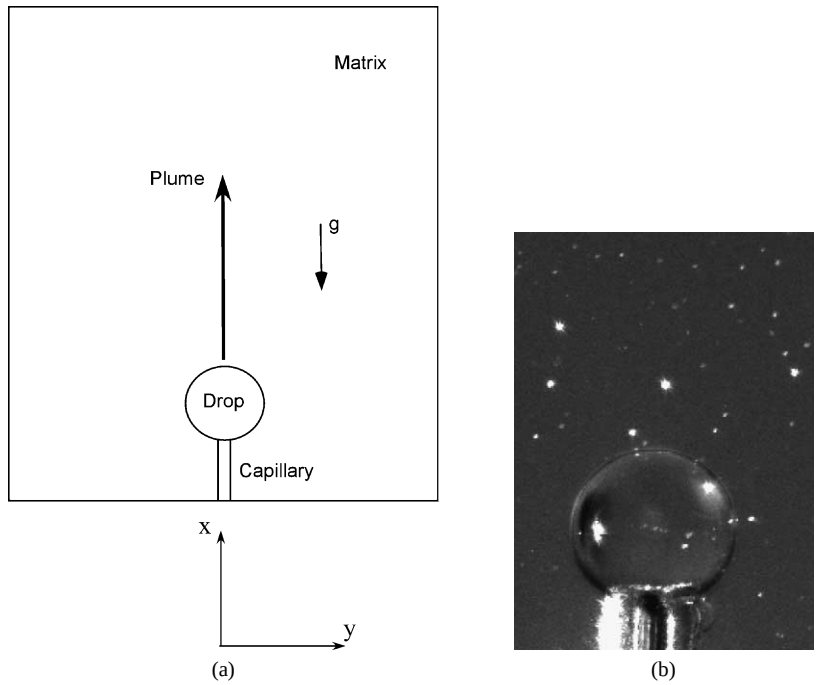

Fig. 2. (a) Sketch of the geometrical configuration; (b) liquid drop at the tip of the capillary tube.

used for moving boundary problems (Volume of fluid VOF methods, see, e.g., the excellent works of Hirt and Nichols [11], Osher and Sethian [12], Gueyffier et al. [13]). For this reason in the present paper this strategy is adopted.

In the specific case of drops growing or dissolving in a matrix of different liquid, one must generally accomplish at least two things simultaneously: (a) determine the concentration fields in both the liquid phases and (b) determine the position of the interface between the phase 1 and the phase 2.

3.3. DDVF – Volume of Fluid Method for dissolving drops

The DDVF is a single region formulation and allows a fixed-grid solution to be undertaken. It is therefore able to utilize standard solution procedures for the fluid flow and species equations directly, without resorting to mathematical manipulations and transformations.

The model is based on the mass balance equations. The diffusion of the species is governed by the equations (drop = phase $1 \rightarrow \phi = 1$, matrix = phase $2 \rightarrow \phi = 0$):

$$\frac{\partial C_1}{\partial t} = \phi\left[-\underline{\nabla} \cdot (\underline{V} C_1) + D\nabla^2 C_1\right], \tag{1}$$

$$\frac{\partial C_2}{\partial t} = (1-\phi)\left[-\underline{\nabla} \cdot (\underline{V} C_2) + D\nabla^2 C_2\right], \tag{2}$$

where D is the interdiffusion coefficient.

The species equations (1) and (2) are solved throughout the computational domain including the drop and the matrix. The presence of the terms ϕ and $1-\phi$ ensures in fact that each equation characterizes a different phase. At the initial instant both the phases are supposed to be at constant concentration ($C_{1(\mathrm{o})}$ and $C_{2(\mathrm{o})}$, respectively).

The behaviour of the two phases is coupled through the equilibrium concentration values imposed on the two sides of the interface. These values come from the miscibility law (see Fig. 1 and [14]) according to the local value of the temperature of the interface (for isothermal conditions of course the equilibrium values are constant along the interface). At the interface ($0 < \phi < 1$), the concentrations must satisfy the equilibrium conditions:

$$C_1|_i = C_{1(\mathrm{e})}(T), \tag{3}$$

$$C_2|_i = C_{2(\mathrm{e})}(T), \tag{4}$$

i.e., the equilibrium Methanol concentrations at the consolute points of the miscibility diagram (when a drop of pure Methanol is injected into the Cyclohexane liquid matrix, it is assumed that equilibrium at the liquid–liquid interface is attained instantaneously, Perez de Ortiz and Sawistowski [15]). Eqs. (3) and (4) behave as 'moving boundary conditions'.

Note that in place of the 'sharp' transition from one phase to the other that would characterize the multiple region formulations (in that case the interface separating the bulk phases is a mathematical boundary of zero thickness), here the phase-field varies smoothly but rapidly through an interfacial region whose thickness is not zero. This region, defined by the mathematical conditions $|\underline{\nabla}\phi| \neq 0,\ 0 < \phi < 1$, moves through the computational domain according to the behaviour of the different phases (i.e., according to the behaviour of ϕ).

The flow is governed by the continuity, and Navier–Stokes equations:

$$\underline{\nabla} \cdot \underline{V} = 0 \tag{5}$$

$$\frac{\partial(\rho \underline{V})}{\partial t} = -\underline{\nabla} p - \underline{\nabla} \cdot [\rho \underline{V}\,\underline{V}] + \underline{\nabla} \cdot [\mu \underline{\nabla}\,\underline{V}] + \underline{F}_g, \tag{6}$$

where

$$\rho = \rho_{1(o)}\phi + \rho_{2(o)}(1-\phi), \tag{7a}$$

$$\mu = \mu_1\phi + \mu_2(1-\phi) \tag{7b}$$

and in the last term of Eq (6):

$$F_g = g\big[\beta_{C1}(C_1 - C_{1(o)})\big]\phi + g\big[\beta_{C2}(C_2 - C_{2(o)})\big](1-\phi) + \rho g\big[\beta_{T1}(T - T_{(o)})\big]\phi + \rho g\big[\beta_{T2}(T - T_{(o)})\big](1-\phi) \tag{7c}$$

the Boussinesque approximation is used to model the buoyancy forces, β_{C1} and β_{C2} are the solutal expansion coefficients related to the mutual interpenetration of the phases 1 and 2, β_{T1} and β_{T2}, the thermal expansion coefficients.

The temperature distribution is governed by the energy equation:

$$\frac{\partial \rho C_P T}{\partial t} = \big[-\underline{\nabla} \cdot (\rho C_P \underline{V} T) + \underline{\nabla} \cdot (\lambda \underline{\nabla} T)\big], \tag{8}$$

where the thermal conductivity λ and the specific heat C_P are computed as

$$\lambda = \lambda_1\phi + \lambda_2(1-\phi), \tag{9a}$$

$$C_P = C_{P1}\phi + C_{P2}(1-\phi). \tag{9b}$$

The core of the DDVF method is its technique for adjourning ϕ. The tracking of the interface between the phases is accomplished by the solution of a special continuity integral equation for the volume of the liquid drop taking into account the release or absorption of solute through the interface (the liquid drop is assumed to be a sphere of radius R increasing due to growth or decreasing due to dissolution).

With regard to the aforementioned equation, it should be pointed out that in principle if a "Lagrangian" (i.e., moving with the "interface") reference frame is assumed to describe the behaviour of the droplet phase that dissolves within the (miscible) matrix, mass balance simply requires that the diffusive solutal fluxes computed at the two different sides of the drop surface must be equal, i.e., the aforementioned equation would read $J_1 = J_2$.

Since the interface moves with a velocity ζ through the reference frame, the overall jump mass balance reads $\delta[\rho(V_n - \zeta)] = 0$ where V_n is the fluid velocity component orthogonal to the free surface. Assuming $\rho_1 \cong \rho_2$ (see Table 1) the above equation reduces to $(V_{n1} - \zeta) = (V_{n2} - \zeta) \rightarrow V_{n1} = V_{n2}$. Moreover $V_n = 0$ on both sides of the interface since there is not any local macroscopic convective transport of fluid across the drop surface (the inward or outward motion of the interface being only based on molecular diffusion). Thus the jump specie balance equation $\delta[\rho(V_n - \zeta)C - \rho D \partial C/\partial n] = 0$ reads (see also Bassano [10]):

$$-D\left.\frac{\partial C_2}{\partial n}\right|_i + C_2|_i \dot{m} = -D\left.\frac{\partial C_1}{\partial n}\right|_i + C_1|_i \dot{m}. \tag{10a}$$

Where $\dot{m}$ is the mass flow rate through the interface (n points towards the matrix; if the drop dissolves, $\dot{m}$ is positive and ς is negative, i.e., $\dot{m} = -\zeta$ with $\zeta \cong \mathrm{d}R/\mathrm{d}t$); therefore

$$D\left(\left.\frac{\partial C_2}{\partial n}\right|_i - \left.\frac{\partial C_1}{\partial n}\right|_i\right) = \zeta\,\Delta C \quad \text{with } \Delta C = C_1|_i - C_2|_i. \tag{10b}$$

In conclusion integrating over the surface of the drop, one obtains for the time evolution of the radius:

$$\frac{\mathrm{d}R}{\mathrm{d}t} = D\frac{1}{S}\oint \frac{1}{C_1|_i - C_2|_i}\left(\left.\frac{\partial C_2}{\partial n}\right|_i - \left.\frac{\partial C_1}{\partial n}\right|_i\right)\mathrm{d}l, \tag{10c}$$

Table 1
Physical properties

D [$m^2\,s^{-1}$]	2×10^{-9}
ρ_1 [$Kg\,m^{-3}$]	0.782×10^{3}
ρ_2 [$Kg\,m^{-3}$]	0.769×10^{3}
ν_1 [$m^2\,s^{-}1$]	1.03×10^{-6}
ν_2 [$m^2\,s^{-1}$]	1.275×10^{-6}
β_1 [–]	4.62×10^{-2}
β_2 [–]	-4.95×10^{-2}
β_{T1} [K^{-1}]	1.14×10^{-3}
β_{T2} [K^{-1}]	1.14×10^{-3}
C_{P1} [$J\,Kg^{-1}\,K^{-1}$]	2.51×10^{3}
C_{P2} [$J\,Kg^{-1}\,K^{-}1$]	1.86×10^{3}
λ_1 [$J\,m^{-1}\,s^{-1}\,K^{-1}$]	2.02×10^{-1}
λ_2 [$J\,m^{-1}\,s^{-1}\,K^{-1}$]	1.25×10^{-1}
σ_T [$dyne\,m^{-1}\,K^{-1}$]	17.42

where S is the surface of the drop, and

$$\frac{\partial C}{\partial n} = \underline{\nabla} C \cdot \underline{\hat{n}} = \alpha \frac{\partial C}{\partial x} + \beta \frac{\partial C}{\partial y}, \tag{11}$$

$$\underline{\hat{n}} = -\frac{\underline{\nabla}\phi}{|\underline{\nabla}\phi|} = (\alpha, \beta), \tag{12}$$

$$\alpha = -\frac{\partial \widehat{\phi}}{\partial x} \Big/ \sqrt{\left(\frac{\partial \widehat{\phi}}{\partial x}\right)^2 + \left(\frac{\partial \widehat{\phi}}{\partial y}\right)^2}, \qquad \beta = -\frac{\partial \widehat{\phi}}{\partial y} \Big/ \sqrt{\left(\frac{\partial \widehat{\phi}}{\partial x}\right)^2 + \left(\frac{\partial \widehat{\phi}}{\partial y}\right)^2}. \tag{13}$$

The unit vector $\underline{\hat{n}}$ perpendicular to the interface results from the gradient of a smoothed phase field $\widehat{\phi}$, where the transition from one phase to the other takes place continuously over several cells (typically 4 or 5 for a grid having 200×200 points). The smoothed phase field $\widehat{\phi}$ is obtained by convolution of the unsmoothed field ϕ with an interpolation function. The interface orientation depends on the direction of the volume fraction gradient of the phase $\widehat{\phi}$ within the cell, and that of the neighbour cell (or cells) sharing the face in question. Depending on the interface's orientation and on the side (phase 1 or phase 2) on which computations are performed, concentration gradients are discretized by forward or backward schemes. After the computation of the radius at the new instant $n+1$, then the distribution of the phase variable ϕ is re-initialized to take into account the volume change, i.e., $\phi = 1$ for $r < R$ and $\phi = 0$ for $r > R$.

Eqs. (1), (2), (5), (6), (8) and (10c) represent a system of five partial differential equations and one ordinary differential equation whose solution governs the non-linear behaviour of the physical system under investigation.

Note that the present mathematical model and related numerical technique can be seen as a very hybrid volume of fluid method.

In the "classical" VOF methods, the phase field variable ϕ is 'advected' solving an appropriate partial differential transport equation; this formulation has been often used for the solution of typical problems dealing with the migration of bubbles or drops posed in liquids. It relies on the fact that the fluids are not interpenetrating. For the present method the equation governing the evolution of ϕ comes from mass balance conditions rather than from transport. Moreover interpenetration of the different fluids is allowed according to the coupled behaviour of Eqs. (1), (2) and (10c).

Furthermore Eq. (10c) provides the necessary coupling among the species and momentum equations. The density and the dynamic viscosity of the liquid in Eq. (6) in fact are computed according to the instantaneous distribution of ϕ. Additional coupling between the species and momentum equations is due to the volume force term (Boussinesque approximation) in Eq. (6).

The Marangoni condition at the drop interface reads (hereafter V_S and V_n denote the velocity components in the plane (x, y) parallel and orthogonal to the free surface, respectively):

$$\mu_1 \frac{\partial V_s}{\partial n}\bigg|_1 - \mu_2 \frac{\partial V_s}{\partial n}\bigg|_2 = \sigma_T \frac{\partial T}{\partial s}, \tag{14}$$

where $V_s = \beta u - \alpha v$ (u and v are the velocity components along x and y, respectively) and

$$V_n = \alpha u + \beta v = 0, \tag{15}$$

$$\frac{\partial V_s}{\partial n} = \alpha \frac{\partial V_s}{\partial x} + \beta \frac{\partial V_s}{\partial y}, \tag{16}$$

$$\frac{\partial T}{\partial s} = \beta \frac{\partial T}{\partial x} - \alpha \frac{\partial T}{\partial y}. \tag{17}$$

Depending on the interface's orientation and on the side (phase 1 or phase 2) on which computations are performed, gradients are discretized by forward or backward schemes.

Eq. (14) with Eqs. (15)–(17) allows the computation of the u and v components satisfying the Marangoni shear stress balance along the drop surface.

The parameter σ_T in Eq. (14) is the derivative of the surface tension with respect to the temperature (for further details see Warren and Webb [16]). The physical properties of the system are shown in Table 1.

Eqs. (1), (2), (5), (6), (8) have been solved with the SMAC method. The method is not described here for the sake of brevity and since it is well known. For further details see, e.g., [3] and [17–19]. A grid 300×100 ($N_x \times N_y$) has been used to ensure good resolution and grid-independence. According to the structure of the convective phenomena under investigation, the computations are axi-symmetric.

4. Results and discussion

First the attention is focused on the case of isothermal configuration, then the presence of a temperature gradient is discussed and compared with the isothermal condition. It is worthwhile to stress how in the case of temperature constant throughout the system, the onset of Marangoni stresses at the drop surface is prevented. In this case in fact neither temperature nor solutal gradients can exist at the interface separating the fluids (the equilibrium concentration values outside and inside the droplet, respectively, are constant along the surface). The comparison between isothermal and non-isothermal conditions, allows to discern the role played by the Marangoni effect in the dissolution process and on the underlying convective mechanisms.

4.1. The solutal plume in isothermal conditions

According to the experimental results, if a droplet of Methanol is formed on the tip of a capillary immersed into the Cyclohexane, in spite of the small differences in density between the drop and the surrounding matrix, a convective plume is clearly observed; the plume originates at the tip of the drop and is directed upward (Fig. 3).

In previous experiments with different liquid–liquid systems (Aniline/Water, Isobutanol/Water, Ethilacetate/Water, see Agble and Mendes Tatsis [20]) similar convective plumes were observed. In the above mentioned studies, the systems basically consisted of sitting drops or of pendant drops. It was shown that the convective plume originated from the drop is directed downward or upward according to whether the liquid is heavier or lighter than that used for the matrix.

For the system under investigation, the droplet (Methanol) is heavier than the surrounding matrix. Nevertheless a rising convective plume is observed at the dissolving liquid–liquid interface.

This phenomenon can be explained by the particular density dependence as function of the concentration for the Cyclohexane–Methanol system. According to the literature (Ref. [14]), the density of the Cyclohexane–Methanol binary mixture can be a decreasing or an increasing function of the Methanol concentration depending on the concentration range. The density is a decreasing function of the Methanol concentration for $0 < c < c_1$, whereas it is an increasing function of c for $c_2 < c < 1$ ((c_1 and c_2 are the Methanol concentrations at the consolute points of the miscibility diagram, see Fig. 1). When a drop of pure Methanol is injected into the Cyclohexane liquid matrix, equilibrium at the liquid–liquid interface is attained instantaneously (Perez de Ortiz and Sawistowski [15]). Assuming negligible thermal effects (an average temperature of 25 [°C] and temperature differences less than 0.2 [°C] were measured with thermocouples), according to the phase rule the concentrations at the interface will be c_1 and c_2(outside and inside the droplet, respectively, see Fig. 1). Correspondingly the mixture surrounding the droplet is lighter than the external matrix and therefore a rising plume is originated (Fig. 4).

After an initial transient time, a quite stable buoyant rising jet continuously carrying Methanol towards the top of the test cell is created.

4.2. Non-isothermal conditions

If a temperature gradient ($\partial T/\partial x$) is applied to the liquid matrix, by heating the top of the test cell and cooling the bottom, the regular release of Methanol in the rising jet discussed above, is taken over by a new spatio-temporal behaviour.

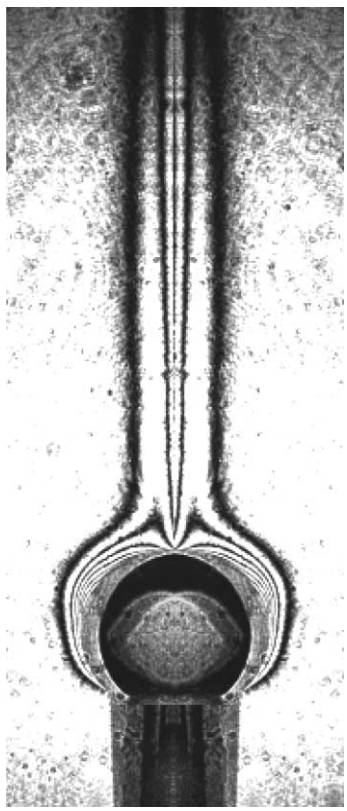

Fig. 3. Rising plume from a droplet of Methanol dissolving in Cyclohexane (uniform temperature distribution $T = 25$ [°C], initial drop volume 3 [μl]): experimental results.

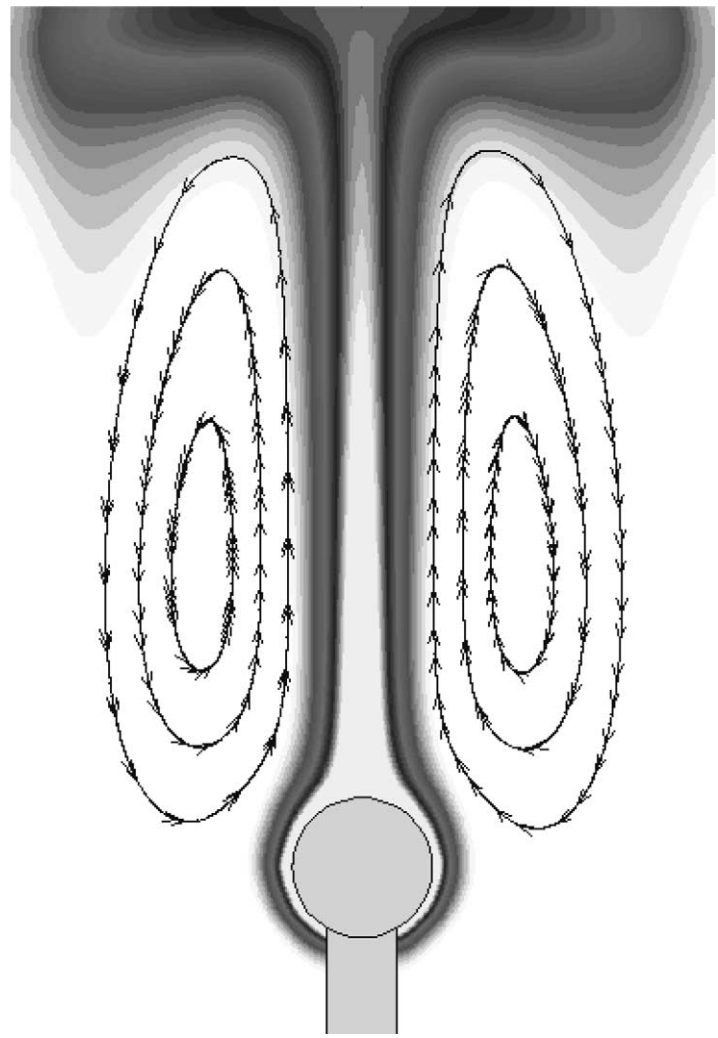

Fig. 4. Rising plume from a droplet of Methanol dissolving in Cyclohexane (uniform temperature distribution $T = 25$ [°C], initial drop volume 3 [μl]): numerical results.

For sufficiently small values of the temperature gradient ($\partial T/\partial x$), the transport of Methanol in the rising jet is similar to that obtained in the case of isothermal conditions, but if $\partial T/\partial x$ exceeds a certain critical value (for instance for a droplet having initial volume 3 [μl], the critical $\partial T/\partial x$ is about 1 [K cm^{-1}]), the aforementioned mechanism undergoes a transition to an oscillatory axi-symmetric complex flow pattern.

Instead of a steady regular plume, release of solute occurs in the form of discrete events separated by certain time (and thus space) intervals. The instability in fact leads somehow to a "periodic shooting" of a "packet" of lighter fluid in the surrounding liquid (Fig. 5). This behaviour appears in the form of a couple of curls that are initially formed close to the drop surface and then are transported upward by buoyancy effects. The phenomenon behaves as a disturbance travelling towards the top (i.e., a perturbation of the solutal and flow field periodically rising along the symmetry axis).

These behaviours have been confirmed by the numerical simulations (Fig. 6).

The mathematical model and the associated numerical algorithm have proven to be able to "capture" the complex time-dependent phenomena and to elucidate some experimental behaviours. For instance the numerical simulations (Fig. 6) show that the curls in the interference fringes pattern correspond to the presence of a toroidal convection roll periodically released at the peak of the dissolving drop.

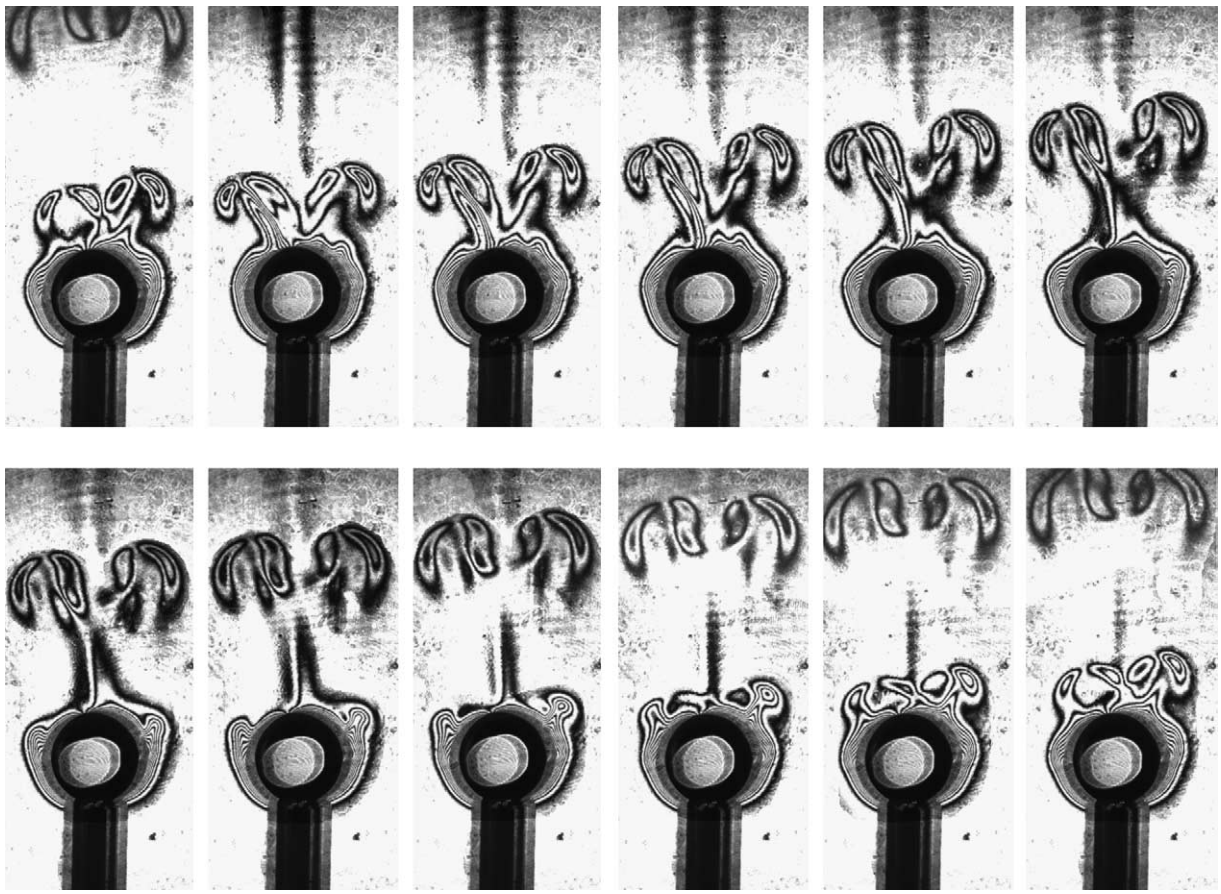

Fig. 5. Experimental results: oscillatory instability of the axisymmetric plume rising from a drop of Methanol dissolving in a Cyclohexane matrix with $\partial T/\partial x = 2.3$ [°C cm^{-1}] ($T_{\text{average}} = 27$ [°C]). The initial volume of the drop is 3 [μl]. The images are taken at time intervals of about 1 seconds. One period of the oscillating behaviour is shown.

The experimental and numerical frequencies exhibit a satisfactory agreement (see Table 2); the difference (O(20%)) could be explained according to the fact that many physical parameters (in particular the surface tension derivative with respect to the temperature), are still characterized by a large uncertainty (up to 100%) in literature. Also the dependence of the diffusivity on the concentration could be an important reason for the discrepancy between the model prediction and the experimental results. With regard to this aspect it is also worthwhile to stress how, unfortunately, there is still a disappointing lack of information dealing with the value of the diffusion coefficient for the couple Methanol–Cyclohexane. A reliable experimental valuation of this coefficient is not possible on ground due to the inevitable onset of fluid convection; moreover microgravity-based measurements are still not available.

4.3. The nature of the instability

Computations obtained "switching off" surface tension effects, have proven that the presence of the Marangoni effect is crucial in determining this kind of flow instability. In absence of Marangoni effect the solutal jet is not broken into discrete events and the aforementioned characteristic curls do not appear.

It is well known that Marangoni forces drive liquid from hot regions towards cold regions. Accordingly, on the surface of the drop, Marangoni effects tend to drive liquid towards the bottom. On the contrary solutal buoyancy effects act in the opposite direction. Therefore, if the test cell is heated from above and cooled from below, thermal Marangoni and solutal buoyancy flow counteract.

In view of these arguments and according to the fact that the instability does not appear if the surface tension forces are artificially neglected in the simulations, a theory based on the delicate balance of the aforementioned counteracting phenomena could be proposed to explain the oscillatory behaviour.

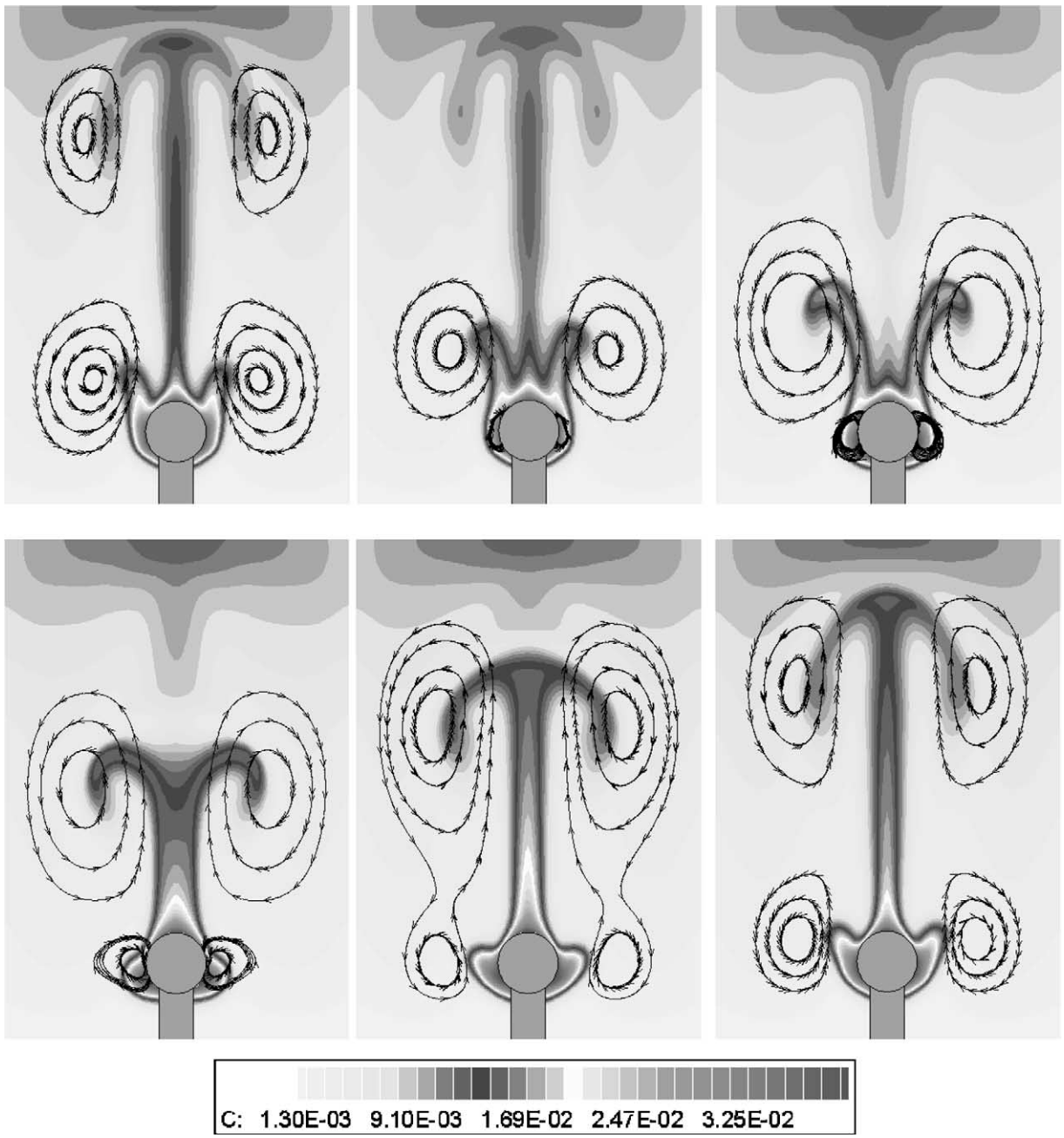

Fig. 6. Computed evolution of the unstable solutal plume: concentration and flow field patterns for a 3 [μl] droplet of Methanol dissolving into a matrix of Cyclohexane with $\partial T/\partial x = 2.3$ [°C cm^{-1}] ($T_{\text{average}} = 27$ [°C]). One period of the oscillating behaviour is shown (the period τ has been divided into 6 parts and the concentration and velocity fields are shown in figures a–f corresponding to $t = 0, \tau/6, \tau/3, \tau/2, 2\tau/3, 5\tau/6$ respectively with $\tau \cong 19$ [s]).

A particular procedure has been used to get insights into these aspects. The basic approach used for this purpose relies on the combination of the available experimental and numerical results with theoretical models. First the trends in available data have been used to postulate qualitatively mechanical principles for explaining the instability (for the case under investigation the aforementioned delicate balance between solutal buoyancy forces and Marangoni thermal stresses). Then, on the basis of the foregoing principles, explicit laws have been proposed and "tested" for their ability to predict the experimentally-determined patterns of the instability threshold.

Table 2
Critical frequency as a function of the initial droplet volume

Volume [μl]	Freq. exp. Res [Hz]	Freq. num. Res [Hz]
1	5.55×10^{-2}	5.88×10^{-2}
3	5.21×10^{-2}	4.76×10^{-2}
5	4.54×10^{-2}	3.84×10^{-2}

This approach in particular has required a very demanding (quite lengthy) parametric analysis about the effect of the initial volume of the droplet. A "scaling" analysis in fact has been carried out to discern the theoretical relationship between the critical temperature gradient and the initial radius of the droplet. See in the detail the discussion below.

If actually the instability follows from a delicate counteracting behaviour between solutal buoyancy and thermal surface-driven effects, it should be possible to draw information about the critical threshold simply imposing that:

Intensity of Solutal buoyancy effects/Intensity Marangoni thermal effects $= \mathrm{O}(1)$.

The relative importance of these effects can be estimated comparing the relevant characteristic velocities.

The solutal buoyancy velocity reads:

$$V_g^C = \frac{g\beta_{C2}\Delta C(2R)^2}{\nu}, \tag{18}$$

where ΔC is the initial concentration difference between the drop surface and the top of the test cell (for the present case $\Delta C \cong C_{2(\mathrm{o})}$).

The thermal Marangoni velocity reads:

$$V_{Ma}^T = \frac{\sigma_T(\partial T/\partial x)2R}{\mu}. \tag{19}$$

Therefore, according to the foregoing arguments the conditions for the onset of the oscillatory instability should correspond simply to

$$\frac{V_{Ma}^T}{V_g^C} = \mathrm{O}(1), \tag{20a}$$

$$\rightarrow \frac{\partial T}{\partial x} \propto \frac{g\beta_C\rho\Delta C}{\sigma_T}2R = \frac{g\beta_{C2}\rho\Delta C}{\sigma_T}2\sqrt[3]{\frac{3}{4\pi}Vol.} \tag{20b}$$

Eq. (20b) is the aforementioned analytical relationship between the critical gradient and the droplet diameter provided by the theoretical scaling analysis carried out under the assumption that the instability is caused by the opposition of the surface Marangoni stress to the natural direction in which the fluid wants to move (upward, because of buoyancy). This explicit law shows that the critical $\partial T/\partial x$ is an increasing function of the initial volume of the droplet.

To provide physical validation to these arguments, Eq. (20b) has been compared with numerical and experimental results carried out on purpose. The comparison shows that the relationship herein presented fits the dependencies highlighted by the experimental and numerical results (Fig. 7).

The consistency of model predictions with experimental data suggests that rate-controlling steps have been taken into account, and that simplifications do not distort actual behaviour. The proposed theory about the counteracting interplay of surface tension and buoyancy forces exhibits quite exhaustive capabilities to predict and elucidate experimental observations (in particular the behaviour of the system as a function of the initial droplet volume) and to identify cause-and-effect relationships, i.e., to give insights into the mechanisms driving the phenomena under investigation.

If the temperature gradient is sufficiently small, buoyancy effects prevail and the velocity along the drop surface is upward (i.e., directed from the capillary towards the point at the peak of the drop). In this case release of solute occurs in the form of a continuous rising jet of lighter liquid starting at the peak of the Methanol drop.

If the temperature gradient is increased, correspondingly, the relative importance of the surface Marangoni stress with respect to local buoyancy forces increases. The $\partial T/\partial x$ at which the aforementioned counteracting effects can be considered competitive in determining the direction of the surface flow, corresponds to the "critical conditions" for the onset of the instability. For temperature differences larger than the critical one, a "back and forth" mechanism occurs, i.e., an instability of the mixed buoyancy-Marangoni type.

This explains why the instability occurs only if a certain initial value of the temperature gradient is exceeded whereas the flow exhibits quite stable solutal rising plumes in the case of small initial ΔT or isothermal conditions. Finally the generation of "curls" close to the drop surface is strictly related to the counteracting behaviour of buoyancy and surface tension forces that lead to the production of vorticity.

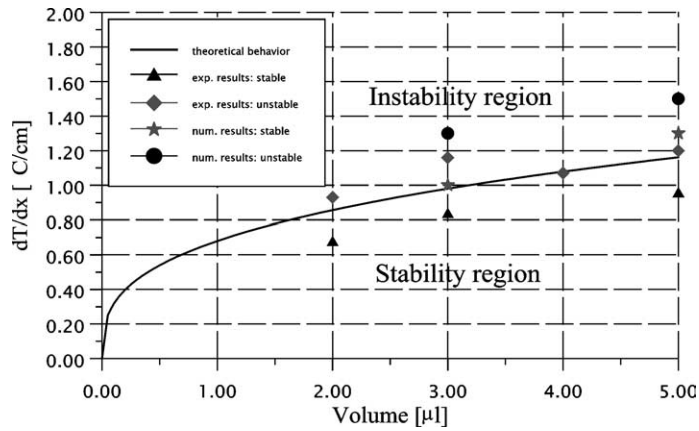

Fig. 7. Stability map and critical temperature gradient ($\partial T/\partial x$) as a function of the initial droplet volume (numerical and experimental results).

It is worthwhile to stress how the behaviours discussed above are heretofore unseen and represent an original contribution to the fluid-dynamics of drops in liquid–liquid systems (fundamental research) as well as to the field of material (alloy) science.

4.4. Comparison with other results available in literature

The literature on the convective instability of jets is very rich. For instance, many analyses have appeared dealing with liquid/gas or liquid/vacuum systems (i.e., the case of liquid jets falling in an ambient gas or in vacuum). For these cases, the commonly observed manifestation of the onset of instability in a liquid jet with a sufficiently large velocity is the amplification of disturbances which are convected downstream to break up the jet into drops. This instability belongs to a general class of instability called "convective instability" which allows the disturbance to be convected only in the downstream direction. The literature on these phenomena is reviewed in many articles including the most recent ones by Chieger and Reitz [21], Lin [22], Lin and Reitz [23]. It is interesting to point out how also another class of instability exists, called "absolute instability" which permits the disturbance to propagate in both the downstream and upstream directions. Leib and Goldstein [24,25] were the first to demonstrate that, also in absence of gravity and ambient gas, a liquid jet with a relatively small velocity may become absolutely unstable and that this behaviour is due to surface tension force. Even in the presence of gas, with (Lin and Lian [26]) or without gas viscosity (Lin and Lian [27]) or compressibility (Zhou and Lin [28]), the absolute instability can occur.

These behaviours have been the focus of intense investigation to develop recommendations on how to avoid unwanted hydrodynamic phenomena for the free surface of free-falling liquid metal jets in a vacuum, which are used for the design of fusion reactors. The undesirable "hydrodynamic behaviours" consists in excess rippling (formation of surface tension waves), deformation of the falling jet and "droplet ejection" at its surface (drops of liquid metal may be ejected from the jet free surface due to turbulent disturbances and shear instabilities); recommendations have been developed by qualitative understanding of the physical mechanisms that cause these phenomena (see the excellent papers of Wu and Miranda [29], Konkachbaev and Morley [30], Soderberg and Alfredson [31], Wu and Faeth [32]).

The present analysis deals with a quite different topic (rising solutal plumes in a liquid/liquid system) so that the aforementioned studies are of little help in elucidating the related mechanisms. Some remarkable analogies however exist with respect to the gas/gas systems that have been studied by Cetegen and his co-workers. "Typical" instabilities of "rising" buoyant jets were investigated by these authors for a number of different cases and fluid-fluid systems (e.g., candle flames and buoyant plumes).

For instance Cetegen [33] carried out experimental studies dealing with the instabilities and flow transitions of buoyant plume/jets of gas mixtures. The author investigated the case of a buoyant plume of helium or helium/air mixture originating from a large axi-symmetric nozzle with low velocity. He found toroidal vortex formation as a result of rapid buoyant acceleration of light plume fluid in heavier more or less quiescent surroundings.

It was found that these plumes may undergo periodic oscillations: as the buoyant fluid exits the nozzle, plume boundary contracts towards the plume centreline as a result of buoyant acceleration due to the hydrostatic pressure field and the condition imposed by the conservation of mass; the plumes undergo periodic oscillations of the plume boundary starting in the immediate vicinity of the nozzle lip. This behaviour might resemble that observed in the present study about the periodic release of "curls" close to the drop surface.

Moreover, in analogy with the present case of solutal plumes, it was found experimentally by Cetegen [33] that not all buoyant plumes exhibit periodic oscillations. The onset of oscillations is, in general, a function of nozzle diameter, nozzle exit

velocity and the density ratio between the plume fluid and its surrounding (Cetegen [33]) as for the present case, instability occurs only if a critical temperature gradient is exceeded.

Cetegen and Kasper [34] provided a very interesting explanation of their observations: the mechanism leading to the periodic oscillatory state of the flow field is connected with the highly unstable (Rayleigh–Taylor) density stratification in the sharply contracting region of the flow just above the nozzle exit.

Important similarities can be found also about the behaviour of "pool fires". It is well known (Cetegen and Ahmed [35]) that axi-symmetric pool fires exhibit a periodic oscillatory motion close to their origin, often referred to as "puffing". In a fire, these periodic oscillations result in formation of large-scale (of the order of burner diameter) flaming vortical structures at a short distance from the burner surface. These structures significantly modify the downstream flame behaviour as they rise through the flame and finally burnout near the flame top.

Again the behaviour is very similar to that observed in the case of the periodic "release" of packets of fluid above the dissolving drop. The perturbation in the concentration field originated at the drop surface rises along the core of the jet and dies at the top.

It is crucial to point out how, despite the macroscopic analogies and apparent common features, however the cause-and-effect relationships exhibit notable differences with respect to the present case of dissolving drops in non-isothermal conditions.

In the case of isothermal helium plumes and flames the oscillatory behaviour follows from an instability of the "pure" buoyant flow. In particular for helium plumes the force driving the instability is the pressure gradient between the helium reservoir and the ambient. In the case of flames and fires, the driving force is the release of heat in the core of the flame due to the combustion process; puffing in pool fires in fact is typically stronger than buoyant non-reacting plumes due to the local heat release and the consequently maintained buoyancy. These instabilities are hydrodynamic in nature, i.e., bifurcation to oscillatory flow occurs when the velocity in the core of the rising plume exceeds a critical value. Despite the similarities at macroscopic scale the underlying mechanisms for the case of dissolving drop are very different. The related transition to oscillatory flow does not follow from an instability of the rising jet; it is due to a delicate balance between two counteracting effects (buoyancy and surface-tension-driven stresses) at the surface of the dissolving drop (as proven by the numerical computations carried out "switching off" the Marangoni effects).

5. Conclusions

An intriguing behaviour dealing with the dissolution process of a droplet of Methanol in a Cyclohexane matrix has been investigated as a model to study phenomena related to solidification processes involving opaque metal alloys in the liquid state.

In the presence of a temperature gradient, the release of solute in the liquid (matrix) surrounding the droplet is governed by buoyancy and surface tension forces. The delicate balance between these two effects is responsible for the onset of a heretofore unseen instability of the flow field. Instead of a continuous rising jet carrying Methanol towards the top of the test cell, "packets" of solute are periodically shoot upward.

Both experimental observation and numerical modelling show comparable evidences of the phenomena under investigation. The qualitative consistency (in terms of spatio-temporal behaviour) of model predictions with experimental data suggests that rate-controlling steps have been taken into account, and that simplifications do not distort actual behaviour. The code captures the underlying physical mechanisms responsible for the onset of oscillatory instability and the experimental and numerical frequencies are in reasonable agreement. The proposed models and methods allow to predict and elucidate experimental observations and to identify cause-and-effect relationships, i.e., to give insights into the mechanisms driving the phenomena under investigation.

Acknowledgements

The present work has been supported by the European Space Agency (ESA) and the Italian Space Agency (ASI).

References

[1] Decomposition, phase separation, solidification of immiscible liquid alloys, in: L. Ratke (Ed.), Immiscible Liquid Metals and Organics, Proceedings of an International Workshop Organized by the ESA Expert Working Group, "Immiscible alloys" held in the Physikzentrum, Bad Honnef, Germany, 1992, pp. 3–34.

[2] B. Prinz, A. Romero, New casting process for hypermonotectic alloys, in: L. Ratke (Ed.), Immiscible Liquid Metals and Organics, Proceedings of an International Workshop Organized by the ESA Expert Working Group, "Immiscible alloys" held in the Physikzentrum, Bad Honnef, Germany, 1992, pp. 281–289.

[3] R. Monti, R. Savino, M. Lappa, S. Tempesta, Behaviour of drops in contact with liquid surfaces at non wetting conditions, Phys. Fluids 10 (11) (1998) 2786–2796.
[4] R. Monti, R. Savino, D. Paterna, M. Lappa, New features of drops dynamics under Marangoni effect, in: Recent Research Developments in Fluid Dynamics, vol. 3, Transworld Research Network, Trivandrum, India, 2000, pp. 15–32.
[5] P. Dell'Aversana, M. Lappa, G.P. Neitzel, Elasto-hydrodynamic lubrication of ball bearings and drops, in: 2002 APS (Americal Physical Society) Division of Fluid Dynamics 55th Annual Meeting (DFD02), Dallas, TX, November 24–26, 2002, Log 10197.
[6] R. Savino, D. Paterna, M. Lappa, Marangoni flotation of liquid droplets, J. Fluid Mech. 479 (2003) 307–326.
[7] N.O. Young, J.S. Goldstein, M.J. Block, The motion of bubbles in a vertical temperature gradient, J. Fluid Mech. 6 (1959) 350–360.
[8] R.S. Subramanian, R. Balasubramaniam, The Motion of Bubbles and Drops in Reduced Gravity, Cambridge University Press, Cambridge, UK, 2001.
[9] R.S. Subramanian, L. Zhang, R. Balasubramaniam, Mass transport from a drop executing thermocapillary motion, Microgravity Sci. Tech. XII (3/4) (2001) 107–115.
[10] E. Bassano, Numerical simulation of thermo-solutal-capillary migration of a dissolving drop in a cavity, Int. J. Numer. Methods Fluids 41 (2003) 765–788.
[11] C.W. Hirt, B.D. Nichols, Volume of fluid (VOF) method for the dynamics of free boundaries, J. Comput. Phys. 39 (1981) 201–225.
[12] S. Osher, J.A. Sethian, Fronts propagating with curvature-dependent speed: algorithms based on Hamilton–Jacobi formulations, J. Comput. Phys. 79 (1988) 12–49.
[13] D. Gueyffier, J. Li, A. Nadim, S. Scardovelli, S. Zaleski, Volume of fluid interface tracking with smoothed surface stress methods for three-dimensional flows, J. Comput. Phys. 152 (1999) 423–456.
[14] The Physical-Chemical Constants of Binary Systems, Interscience, New York, 1959.
[15] E.S. Perez de Ortiz, H. Sawistowski, Interfacial instability of binary liquid–liquid systems, I. Stability analysis, J. Chem. Engrg. Sci. 28 (1973) 2051–2061.
[16] C. Warren, W.W. Webb, Interfacial tension of near-critical cyclohexane–methanol mixtures, J. Chem. Phys. 50 (9) (1969) 3694–3700.
[17] M. Lappa, Strategies for parallelizing the three-dimensional Navier–Stokes equations on the Cray T3E, Science and Supercomputing at CINECA 11 (1997) 326–340.
[18] M. Lappa, R. Savino, Parallel solution of three-dimensional Marangoni flow in liquid bridges, Int. J. Numer. Methods Fluids 31 (1999) 911–925.
[19] M. Lappa, Growth and mutual interference of protein seeds under reduced gravity conditions, Phys. Fluids 15 (4) (2003) 1046–1057.
[20] D. Agble, M.A. Mendes Tatsis, The effect of surfactants on interfacial mass transfer in binary liquid–liquid systems, Int. J. Heat Mass Transfer 43 (2000) 1025–1034.
[21] N. Chieger, R.D. Reitz, Regimes of jet breakup and breakup mechanisms (physical aspects), in: K.K. Kuo (Ed.), Recent Advances in Spray Combustion: Spray Atomization and Drop Burning Phenomena, vol. 1, AIAA, Reston, 1996, pp. 109–135.
[22] S.P. Lin, Regimes of jet breakup and breakup mechanisms (mathematical aspects), in: K.K. Kuo (Ed.), Recent Advances in Spray Combustion: Spray Atomization and Drop Burning Phenomena, vol. 1, AIAA, Reston, 1996, pp. 137–160.
[23] S.P. Lin, R.D. Reitz, Drop and spray formation from a liquid jet, Annu. Rev. Fluid Mech. 30 (1998) 85–105, Annual Rev. Inc. Palo Alto.
[24] S.J. Leib, M.E. Goldstein, The generation of capillary instability on liquid jet, J. Fluid Mech. 168 (1986) 479–500.
[25] S.J. Leib, M.E. Goldstein, Convective and absolute instability of a viscous liquid jet, Phys. Fluids 29 (1986) 952–954.
[26] S.P. Lin, Z.W. Lian, Absolute and convective instability of a viscous liquid jet surrounded by a viscous gas in a vertical pipe, Phys. Fluids A 5 (1993) 771–773.
[27] S.P. Lin, Z.W. Lian, Absolute instability of a liquid jet in a gas, Phys. Fluids A 1 (1989) 490–493.
[28] Z.W. Zhou, S.P. Lin, Effects of compressibility on the atomization of liquid jets, J. Propulsion and Power 8 (1992) 736–740.
[29] P.K. Wu, R.F. Miranda, Effect of initial flow conditions on primary breakup of nonturbulent and turbulent round liquid jets, Atom. Sprays 5 (1995) 175–196.
[30] A. Konkachbaev, N.B. Morley, Stability and contraction of a rectangular liquid metal jet in vacuum environment, Fusion Engrg. Design 51–52 (2000) 1109–1114.
[31] L.D. Soderberg, P.H. Alfredson, Experimental and theoretical stability investigations of plane liquid jets, J. Mech. B Fluids 17 (5) (1998) 689–737.
[32] P.K. Wu, G.M. Faeth, Onset and end of drop formation along the surface of turbulent liquid jets in still gases, Phys. Fluid 7 (11) (1995) 2915–2917.
[33] B.M. Cetegen, Behaviour of naturally oscillating and periodically forced axisymmetric buoyant plumes of helium and helium–air mixtures, Phys. Fluids 9 (12) (1997) 3742–3753.
[34] B.M. Cetegen, K.D. Kasper, Experiments on the oscillatory behaviour of buoyant plumes of helium and helium–air, Phys. Fluids 8 (11) (1996) 2974–2984.
[35] B.M. Cetegen, T.A. Ahmed, Experiments on the periodic instability of buoyant plumes and pool fires, Combustion and Flame 93 (1993) 157–184.